EBioMedicine 38 (2018) 57–68

Contents lists available at ScienceDirect

EBioMedicine

journal homepage: www.ebiomedicine.com

EBioMedicine
Published by THE LANCET

Research paper

SF3B4 is regulated by microRNA-133b and promotes cell proliferation and metastasis in hepatocellular carcinoma

Zhiyong Liu [a,1], Wei Li [b,1], Yanan Pang [a], Zaixin Zhou [a], Shupeng Liu [c], Kai Cheng [c], Qin Qin [a], Yin Jia [a], Shanrong Liu [a,*]

[a] Department of Laboratory Diagnostics, Changhai Hospital, Second Military Medical University, Shanghai 200433, China
[b] Department of General Surgery, Changzheng Hospital, Second Military Medical University, Shanghai 200003, China
[c] Clinical Trial Center, Changhai Hospital, Second Military Medical University, Shanghai 200433, China

ARTICLE INFO

Article history:
Received 15 July 2018
Received in revised form 26 October 2018
Accepted 26 October 2018
Available online 1 November 2018

Keywords:
SF3B4
HCC
miRNA-133b
Cell proliferation
Metastasis

ABSTRACT

Background: Splicing factor 3b subunit 4 (SF3B4) is a splicing factor and potential oncogene in hepatocellular carcinoma (HCC); however, its regulatory mechanism is yet unclear. We aimed to determine the role of SF3B4 in HCC and the underlying mechanism.
Methods: To investigate the association between alternative splicing events and miRNAs, putative miRNAs were screened using TargetScan. Expression levels of and prognostic information for SF3B4 and miRNAs were determined based on public genomic data and clinical samples. Then, we examined the possible roles of SF3B4 and miRNA-133b in HCC cells and a xenograft mouse model. Pearson correlation analysis and *in vitro* experiments verified SF3B4 as a miRNA-133b target. Protein levels of key targets from the SF3B4 signaling pathway were estimated using western blotting.
Findings: The expression of SF3B4 was upregulated in HCC tissues and cell lines whereas, the expression of miRNA-133b was downregulated. MiRNA-133b negatively regulated the expression of SF3B4. Effects of SF3B4 overexpression were partially abolished by miRNA-133b mimics, confirming that SF3B4 is a target of miRNA-133b. Moreover, molecules associated with SF3B4, including KLF4, KIP1, and SNAI2, were also modulated by miRNA-133b.
Interpretation: SF3B4 plays a crucial role in HCC and is negatively regulated by miRNA-133b. The miRNA-133b/SF3B4 axis may serve as a new therapeutic target for HCC treatment.
Fund: China National Funds for Distinguished Young Scientists (No.81425019), the State Key Program of National Natural Science Foundation of China (No.81730076), Shanghai Science and Technology Committee Program (No.18XD1405300) and Specially-Appointed Professor Fund of Shanghai (GZ2015009). China National Funds for National Natural Science Fund (No.81672899).

1. Introduction

Hepatocellular carcinoma (HCC) is a common type of liver cancer and is one of the most leading fatal malignancies worldwide [1]. Despite advances in surgical approaches and potential therapeutic targets, the prognosis of HCC patients is still poor, notably for those in later stages of the disease [2]. This is mainly because HCC is a complicated disease associated with a variety of genetic and epigenetic mutations. Alternative splicing (AS) is a post-transcriptional gene regulatory mechanism, which produces multiple mRNA isoforms and distinct corresponding protein variants from a single gene, which may play critical roles in the physiological behavior of tumors [3,4]. Abnormal AS events can directly affect tumorigenesis and increase the heterogeneity of HCC [5].

SF3B4 is one of the components of the splicing factor 3b (SF3b) complex [6]. Splicing events are generated through the synergetic actions of multi-subunit complexes. Although SF3B4 mutations frequently result in the Nager syndrome [7,8], the biological roles of SF3B4 in human cancer are only just beginning to be perceived. Prior studies have shown that SF3B4 expression is upregulated in HCC [9,10]. Shen, et al. found that SF3B4 is a crucial HCC marker. As compared with the currently used HCC diagnostic markers, glypican3 (GPC3), glutamine synthetase (GS), and heat-shock protein 70 (HSP70), SF3B4 along with barrier to autointegration factor 1 (BANF1), procollagen-lysine, and 2-oxoglutarate 5-dioxygenase 3 (PLOD3) provides a superior means for the diagnosis of early-stage HCC [11]. As a splicing factor, the exact

* Corresponding author at: Changhai Hospital, Second Military Medical University, 168 Changhai Road, Shanghai 200433, China.
E-mail address: liushanrong@hotmail.com (S. Liu).
[1] These authors contributed equally to this work.

https://doi.org/10.1016/j.ebiom.2018.10.067

Research in context

Evidence before this study

Alternative splicing is a complicated process in tumor development. Prior studies have shown increased expression of SF3B4 as a splicing member in HCC. However, the particular role of SF3B4 and how its expression is upregulated is yet unclear.

Added value of this study

In this study, we initially observed that the expression of SF3B4 is increased in HCC. MiRNA-133b was found upregulate SF3B4 expression. Both, SF3B4 and miRNA-133b play critical roles in HCC. We also found that miRNA-133b regulates the splicing efficiency of SF3B4, and has an impact on the SF3B4 associated signaling pathway.

Implications of all the available evidence

miRNAs play distinct roles in cellular development. Whether miRNAs participate in the process of alternative splicing in HCC or not is poorly understood. This study shows a strong inverse relationship between SF3B4 and miRNA-133b. We provide a novel insight into the miRNA-133b/SF3B4 regulatory axis for the treatment of HCC.

mechanism of SF3B4 upregulation and its specific function in HCC are still unclear.

MicroRNAs (miRNAs) belong to a family of small noncoding RNAs, and are generally about 20 nucleotides long. >2000 mature human miRNAs are known [12]. One of the most important features of miRNAs is that they can bind to the 3′-untranslated region (3′-UTR) of their target mRNAs, and then regulate the expression of their respective target genes [12,13]. Use of *in silico* techniques has revealed that ~60% of human mRNAs might be targets of miRNAs [14]. miRNAs are also known to interact with lncRNAs [15–17]. Thus, miRNAs may be associated with several biological processes such as cell proliferation, apoptosis, and migration [18]. In human cancers, miRNAs function as oncogenes and tumor suppressors when they are aberrantly expressed in different types of tumor tissues [19–21]. However, literature review revealed, limited data showing the association between miRNAs and AS events in tumor biology.

The main purpose of this study was to investigate the specific role of SF3B4 in HCC, and to understand the relationship between miRNAs and AS events mediated by SF3B4.

2. Materials and methods

2.1. Clinical samples

HCC tissues and adjacent non-tumor tissues were obtained from patients with HCC who had received surgical resection, at the Department of Surgery, Changhai Hospital (Shanghai, China). The histopathologic features of clinical samples were confirmed using H&E staining. The use of human tissues in this study was approved by the Research and Ethics Committee of the Changhai Hospital.

2.2. Cell lines and culture

Human HCC cell lines (Huh7, SMMC-7721) and normal liver cell lines (QSG-7701, L-02) were obtained from the Chinese Academy of Sciences Cell Bank, and were cultured in Dulbecco's Modification of Eagle's Medium (Corning, Manassas, USA) supplemented with 10% Fetal Bovine Serum (Gibco, Invitrogen, USA). Cell cultures were maintained at 37 °C in 5% CO_2, in a humidified incubator.

2.3. Public genomic data analysis

To evaluate the expression levels of SF3B4 and miR-133b in a large number of HCC samples, data were obtained from The Cancer Genome Atlas liver hepatocellular carcinoma project (TCGA_LIHC), Gene Expression profiling interactive analysis (GEPIA) [22] and the Gene Expression Omnibus (GEO) database of the National Center for Biotechnology Information (NCBI) (Accession Number: GSE22058). The clinical characteristics of 96 HCC patients from GSE22058 are shown in Table S2 [23]. Expression levels of SF3B4 and miR-133b, as well as the survival information of HCC patients from TCGA are shown in Table S3 and Table S4.

2.4. RNA extraction

Total RNA was isolated from cells and tissues using RNA fast 200 (Fastagen, China) and Trizol (Invitrogen, USA) according to the manufacturer's protocols. Concentration and purity of the total RNA were estimated using NanoDrop1000 (ThermoFisher, USA). Total RNA was stored at −80 °C until analysis was performed.

2.5. Reverse transcription and quantitative PCR

cDNA was synthesized using the PrimeScript™ RT Master Mix kit (TaKaRa, Japan), following the manufacturer's instructions. MicroRNA cDNA was synthesized using the miRcute Plus miRNA First-Strand cDNA Synthesis Kit (TIANGEN BIOTECH, China). Quantitative RT-PCR was performed using LightCycler® 480 II (Roche, Switzerland), using SYBR® Premix Ex Taq™ II (TaKaRa, Japan) according to the manufacturer's instructions. The comparative Ct method was used for relative quantification. GAPDH and U6 were used as endogenous controls for mRNAs and microRNAs respectively. Primer sequences are shown in Table S1.

2.6. Small interfering RNA (siRNA) synthesis, recombinant plasmid construction and transfection

cDNA encoding the CDS of SF3B4 was PCR-amplified using the I-5™ 2× High-Fidelity Master Mix (TsingKe, China), and subcloned into the *Bam*HI and *Xho*I sites of the pcDNA3.1 vector (Invitrogen, USA), the construct was named pcDNA3.1-SF3B4. The 3′-UTR of SF3B4 mRNA containing the sequences complementary to miRNA-133b was amplified using the I-5™ 2× High-Fidelity Master Mix (TsingKe, China), and subcloned into the *Sac*I and *Xho*I sites of the pmirGLO vector (Promega), and the constructs were named pmirGLO-SF3B4 and pmirGLO-SF3B4-mut. The siRNAs specifically targeting SF3B4, and control siRNAs were synthesized by GenePharma (Shanghai, China). The miRNA-133b mimic, inhibitor and negative control were synthesized by GenePharma. HCC cells were transfected with the plasmids, siRNAs or miRNA mimics using Lipofectamine 3000 (Invitrogen, USA) according to the manufacturer's protocol. To produce a lentiviral vector (LV) suppressing SF3B4 expression, LV-shSF3B4 was constructed by Obio (Shanghai, China). We used an empty vector as a negative control and named it LV-Control. Cells were infected with LV-shSF3B4 or LV-Control in the presence of 5 μg/ml Polybrene (Obio, China) and selected with puromycin (1 μg/ml).Primer sequences, siRNAs, shRNAs and miRNA mimics as well as inhibitor sequences are shown in Table S1.

2.7. Immunohistochemistry

Formalin-fixed, paraffin-embedded sections were deparaffinized in xylene, rehydrated in alcohol, and processed as follows. Sections were

incubated with target retrieval solution (Dako), in a steamer for 45 min followed by treatment with 3% hydrogen peroxide solution for 10 min and protein block (Dako, Denmark) for 20 min at room temperature. Sections were incubated overnight in a humid chamber at 4 °C with an antibody against SF3B4 (AV40609, Sigma-Aldrich, 1:400 dilution) and Ki-67 (9449 T, Cell Signaling Technology, 1:400 dilution), followed by incubation with a biotinylated secondary antibody (Vector Laboratories, USA) for 30 min, and the ABC reagent (Vector Laboratories, USA) for 30 min. Immunocomplexes of horseradish peroxidase with target proteins were visualized using the DAB reaction (Dako, Denmark), and sections were counterstained with hematoxylin before mounting. Micrographs of stained sections were taken using OLYMPUS IX73 and acquisition software (Olympus, Japan).

2.8. Dual luciferase reporter assay

The dual luciferase reporter assay was performed to detect whether miRNA-133b directly targets SF3B4. Recombinant plasmids PmirGLO-SF3B4 and pmirGLO-SF3B4-mut along with miRNA-133b mimics, negative control (NC) and empty vector were divided into 6 groups and were transfected into SMMC-7721 cells, separately. Luciferase activity was measured using the Dual-Luciferase Reporter Assay System (KeyGEN BioTECH, China) 48 h after transfection.

2.9. Western blotting analysis

After treatment with recombinant plasmids or siRNAs, cells were washed using cold PBS and lysed on ice with RIPA lysis buffer (NCM Biotech,China) containing a 1% Protease Inhibitor Cocktail (Sigma-Aldrich, USA). Proteins were separated on 4%-20% polyacrylamide gels (GenScript, USA) using SDS PAGE and then transferred onto PVDF membranes (Perkin Elmer Life Sciences, USA). Blots were blocked for 1 h with 5% nonfat dry milk (BioLight BIO, China) and then incubated with the desired primary antibody overnight at 4 °C. The following primary antibodies were used: SF3B4 (Sigma-Aldrich, USA), KLF4 (ABclnoal, China), KIP1 (Cell Signaling Technology, USA), and SNAI2 (Cell Signaling Technology, USA). Blots were incubated with HRP Goat Anti-Rabbit IgG (H + L) (ABclnoal Technology, China), Protein bands were detected using ImageQuant LAS4000 (GE Healthcare, USA). Protein levels were normalized to those of GAPDH (ABclnonal Technology, China).

2.10. Cell proliferation assays

To examine cell proliferation, a total of 3000 cells were seeded into 96-well plates. Cell proliferation was assessed using the Cell Counting Kit-8 (Dojindo Laboratories, Japan) 0, 12, 24, 36, and 48 h after seeding and incubated at 37 °C for 2 h. Optical density (OD) values at 450 nm were evaluated using Thermo Varioskan™ LUX (Thermo Fisher, USA). The absorbance of cell suspensions at each time point were plotted using proliferation curves. EdU immunofluorescence staining was performed using the EdU Kit (Thermo Fisher, USA) according to the manufacturer's protocol. Results were quantified with Image-J software (NIH image, USA).

2.11. Cell migration assay

HCC cells transfected with recombinant plasmids or siRNAs were collected after 24 h. Cells were washed with cold PBS and seeded on the up-chamber of a transwell chamber. DMEM containing 10% FBS was added to the lower chamber as a chemoattractant. After 12–18 h, migrated cells were fixed using 4% paraformaldehyde solution, and then dyed with 0.1% DAPI and counted using OLYMPUS IX73 microscope (Olympus, Japan).

2.12. Wound healing migration assay

HCC cells were scratched with a sterile 200 μl pipette tip corresponding to the reference line drawn in the center of the base of the plate 24 h after transfection. The scratched adherent cells were washed three times with PBS and cultured using serum-free medium. The scratched areas were observed at 0 h and 24 h, respectively.

2.13. Animal studies

Animal studies were approved by the institutional Ethics Committee on Ethics of Biomedicine, Second Military Medical University. LV-Control or LV-shSF3B4 HCC Cells (3×10^6 cells) were injected subcutaneously into the right flanks of 6 male athymic BALB/c nude mice (4 weeks old). Tumor growth was recorded every four days in the following 4 weeks and tumor volume was evaluated using the formula $a \times b^2 \times 0.5$ (where, a = the longest diameter; b = the shortest diameter). To measure lung metastasis assays, LV-Control or LV-shSF3B4 HCC Cells (5×10^6 cells) were injected through the tail vein of 6 male athymic BALB/c nude mice (4 weeks old). The mice were euthanized 5 weeks after injection, and the number of metastatic lung nodules was counted, though the sample size of metastatic nodules was not determined. Hematoxylin and eosin (HE) staining was used to observe the histopathological manifestation of pulmonary metastases in the mouse model.

2.14. Statistical analysis

GraphPad Prism 6.0 was used to analyze the results. Statistical analyses were performed using SPSS (version 17, IBM SPSS). Differences between groups were analyzed using paired or unpaired two-tailed *t*-tests. Data are represented as mean with standard deviation (SD). $^{**}P < .01$, $^{*}P < .05$. A value of $P < .05$ was considered to be statistically significant.

3. Results

3.1. SF3B4 expression is upregulated in tissues and cell lines and indicates poor prognosis

Large cohorts of data from HCC patients were acquired from the NCBI GEO database (GSE22058) (Fig. 1a left) and GEPIA (Fig. 1a right), they show that the expression of SF3B4 in HCC tissues is higher than that in non-tumor tissues. The clinical information of 96 HCC patients from GSE22058 is shown in Table S2 [23]. We then determined the mRNA levels of SF3B4 in 8 independent pairs of clinical HCC tissue specimens and adjacent tissues and obtained similar results from publicly available databases showing that SF3B4 expression levels in tumor tissues are 2.1-fold higher those in adjacent tissues (Fig. 1b). Analysis of SF3B4 expression levels in human immortalized, non-transformed liver cell lines (QSG-7701 and L-02) and HCC cell lines (SMMC-7721 and Huh7), revealed that SF3B4 expression levels in HCC cells are 3.3 fold higher as compared with those in non-transformed liver cells (Fig. 1c). Kaplan–Meier analysis indicated SF3B4 expression levels are high in HCC tissues associated with reduced overall survival time, $P = .00019$ (Fig. 1d). SF3B4 expression levels and survival information of 181 HCC patients are shown in table S3. Immunohistochemistry data showing SF3B4 protein levels in HCC tissues and non-cancerous tissues shows stronger staining density of SF3B4 in HCC tissues (Fig. 1e). These data reveal that SF3B4 is a potential oncogene in HCC, and its increased expression correlates with poor prognosis of HCC patients.

3.2. SF3B4 is a target gene of miRNA-133b in liver cancer cells

To determine the molecular regulators lying upstream of SF3B4 in HCC cells, we used TargetScan. Bioinformatics analysis, which showed

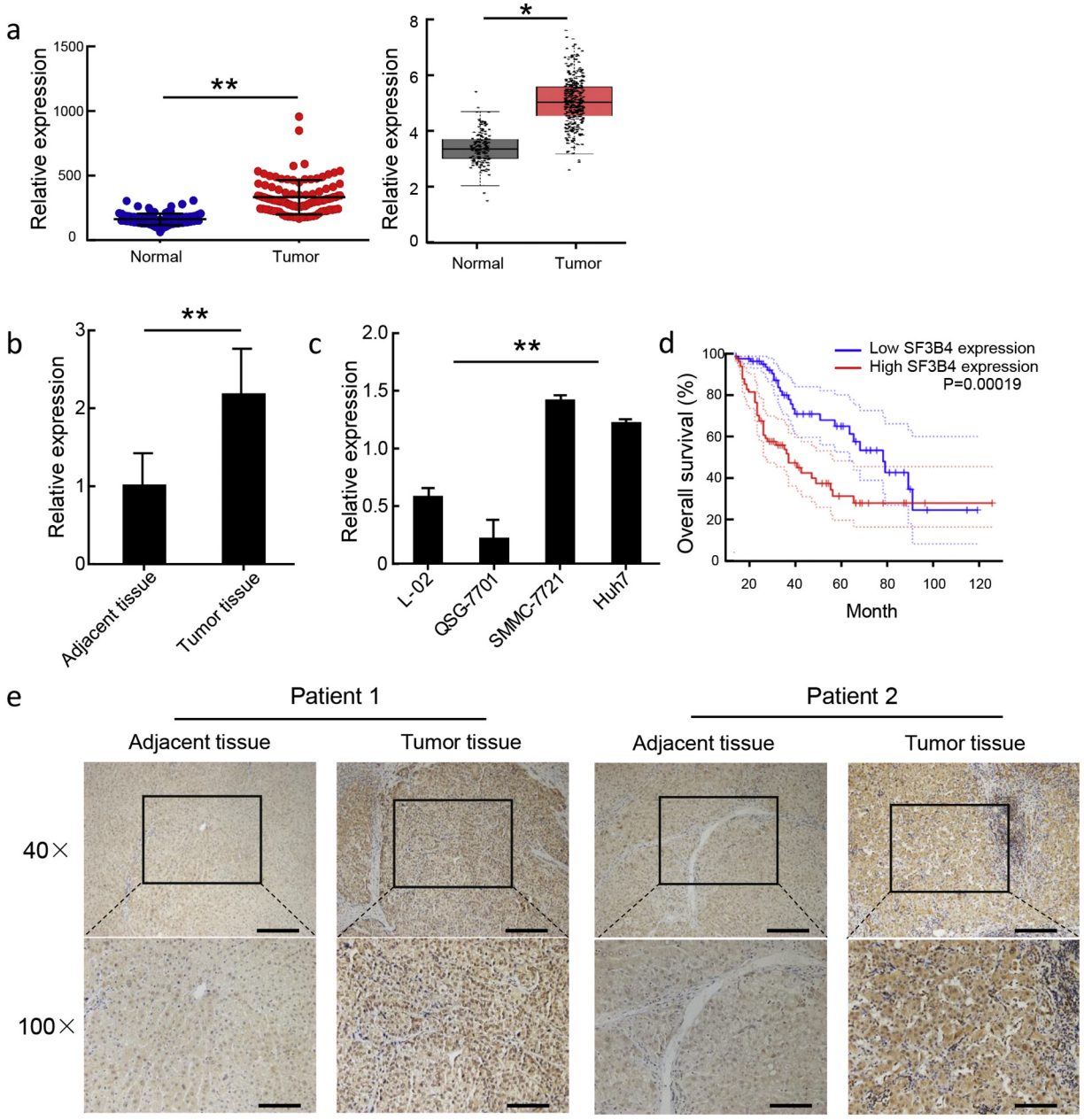

Fig. 1. SF3B4 expression level is increased in HCC. (a) SF3B4 expression level in human HCC tissues and non-cancerous liver tissues from GSE22058 data (left) and GEPIA (right). (b) Real-time qPCR analysis of SF3B4 mRNA level in clinical HCC tissues and adjacent non-tumor hepatic tissues ($n = 8$). (c) Real-time qPCR analysis of SF3B4 mRNA level in HCC cell lines (SMMC-7721, Huh7) and normal liver cell lines (L-02, QSG-7701). (d) Kaplan–Meier analysis of the correlations between SF3B4 mRNA level and recurrence-free survival of 181 HCC patients. (e) Immunohistochemistry (IHC) analysis examining SF3B4 protein level in clinical HCC tissues and adjacent non-tumor hepatic tissues. Scale bars, 100 μm (top), 50 μm (bottom). Data is shown as mean with standard deviation (SD). $^{**}P < .01$, $^{*}P < .05$. Statistical analysis was determined by Student's *t*-test (a, b, c) and Kaplan–Meier analysis (d).

that three miRNAs (miRNA-133b, miRNA-122-5p and miRNA-194-5p) potentially target SF3B4. The 3′-UTR of SF3B4 exists a conserved target region of miRNA-133b (Fig. 2a, Fig. S1a). However, the target regions of miRNA-122-5p and miRNA-194-5p are poorly conserved (Fig. S1b, c). We then examined the expression levels of these three miRNAs in HCC and found that miRNA-133b is downregulated in large cohorts as shown by data from HCC patients (Fig. 2b left), and clinical HCC tissue specimens (Fig. 2b right). Moreover, the expression of SF3B4 mRNA and miRNA-133b in 96 pairs of samples from HCC patient showed a significantly inverse correlation as calculated using Pearson correlation (Fig. 2c). Expression levels of miRNA-122-5p are reduced in HCC tissues (Fig. S1d), however, Pearson analysis showed that miRNA-122-5p and SF3B4 are not significantly related (Fig. S1e). Expression levels of miRNA-194-5p in HCC patients and Pearson correlation analysis showed no significant differences (Fig. S1f, g).

Based on these findings, we selected miRNA-133b as an upstream regulator of SF3B4. Kaplan–Meier analysis indicated that low miRNA-133b expression levels in HCC patients might be associated with poorer overall survival time (Fig. 2d). MiR133b expression levels and survival information of 148 HCC patients from TCGA are shown in table S4. To confirm the relationship between SF3B4 and miRNA-133b, wild-type and mutant SF3B4 3′-UTR sequences were inserted into the pmiRNA-GLO vector (Fig. 2e). Then, a luciferase reporter assay was performed in Huh7 cells. Luciferase activities of wide type SF3B4 in Huh7 cells were much lower than those in control groups (Fig. 2f), this indicated that miRNA-133b directly targets the 3′-UTR of SF3B4. To examine

whether miRNA-133b regulates endogenous SF3B4 expression in HCC cell lines, we transfected miRNA-133b inhibitor, and its mimic into HCC cells (Fig. 2g). mRNA and protein levels of SF3B4 increased nearly 1.5-fold in miRNA-133b knockdown cells than those in the control group. On the contrary, endogenous SF3B4 mRNA and protein levels reduced in Huh7 cells with miRNA-133b overexpression (Fig. 2h). However, altering SF3B4 expression in HCC cells did not affect expression levels of miRNA-133b. These results indicate that miRNA-133b is an upstream regulator of SF3B4, and overexpressing miRNA-133b inhibits the expression of SF3B4 in HCC. Conversely, miRNA-133b knockdown promotes SF3B4 expression.

3.3. SF3B4 deletion shows anti-tumorigenesis effects in vitro and in vivo

To determine the biological functions of SF3B4 in HCC, SF3B4 was knocked down using RNA interference (RNAi), both RNAi-1 and RNAi-2 effectively inhibited SF3B4 expression (Fig. 3a). Cell growth rate was determined using Cell Counting Kit-8 (CCK-8) assays (Fig. 3b). Also,

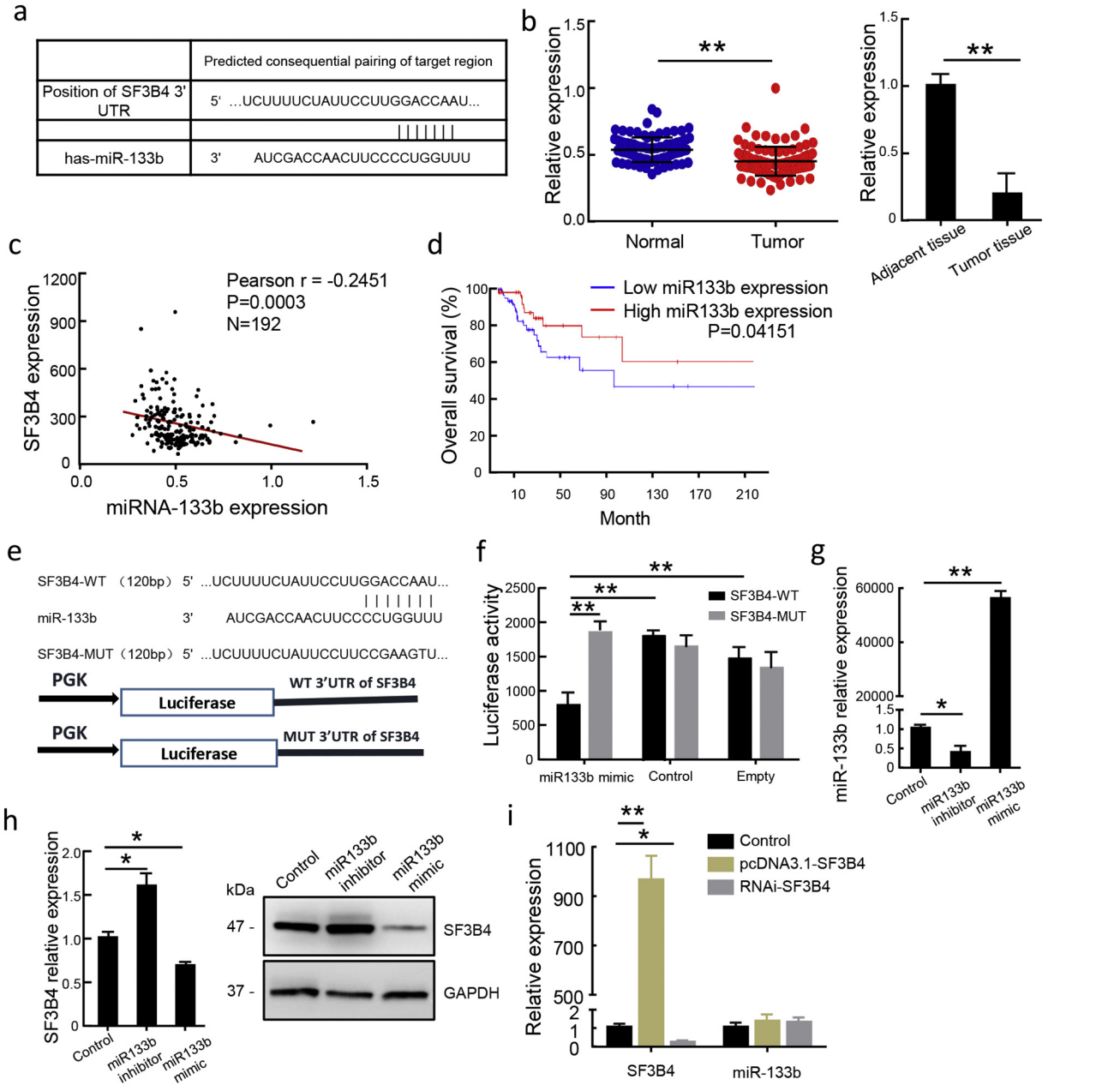

Fig. 2. SF3B4 is a target molecule of miRNA-133b. (a) Sequence of the SF3B4 3'-UTR showing the miRNA-133b binding region. (b) Left, miRNA-133b expression level in human HCC tissues and non-cancerous liver tissues from GSE22058 data. Right, Real-time qPCR analysis of miRNA-133b level in clinical HCC tissues (tumor) and adjacent non-tumor hepatic tissues (liver) (n = 8). (c) The correlation between SF3B4 and miRNA-133b expression level in HCC patients from GSE22058 data ($n = 192$ samples). $P = .0003$, $r = -0.2451$ by Pearson correlation analysis. (d) Kaplan–Meier analysis of the correlations between miRNA-133b level and recurrence-free survival of 148 HCC patients. (e) The WT or MUT SF3B4 3'-UTR was constructed and inserted into the pmir-GLO luciferase reporter vector. (f) The luciferase activity was significantly downregulated in Huh7 cells co-transfected with miRNA-133b mimic and WT SF3B4 3'-UTR vector, but wasn't significantly changed in other groups. Control: Huh7 cells were co-transfected with WT or MUT SF3B4 3'-UTR vector and negative control miRNA. Empty: Huh7 cells were only transfected with WT or MUT SF3B4 3'-UTR vector. (g) The expression levels of miRNA-133b in Huh7 cells transfected with miRNA-133b inhibitor or mimic. (h) The mRNA and protein levels of SF3B4 in Huh7 cells transfected with miRNA-133b inhibitor or mimic. (i) The expression level miRNA-133b when changed the endogenous SF3B4 expression. Data is shown as mean with standard deviation (SD). $^{**}P < .01$, $^{*}P < .05$. Statistical analysis was determined by Student's *t*-test (b, f, g, h, i), Pearson correlation analysis (c) and Kaplan–Meier analysis (d).

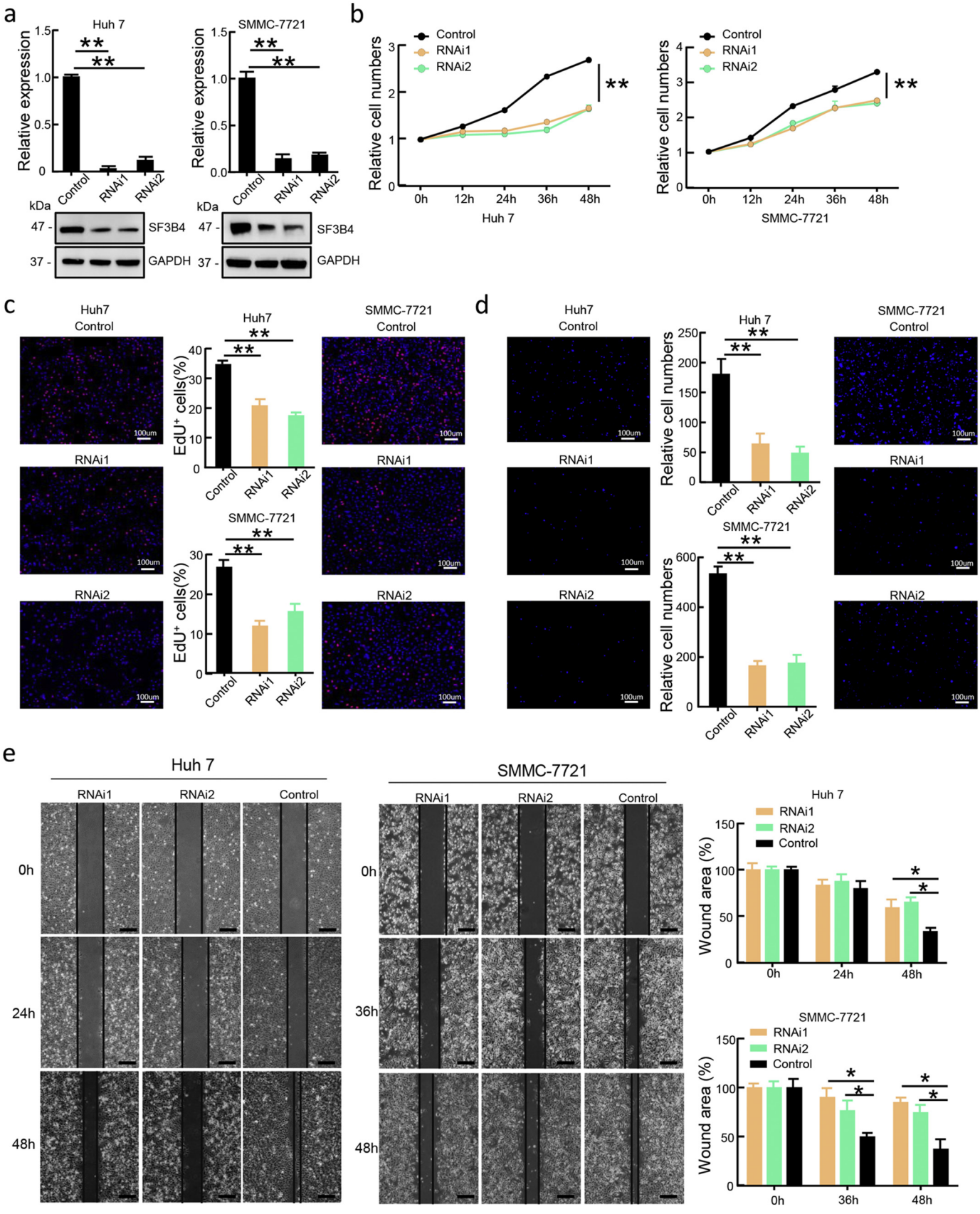

Fig. 3. SF3B4 is required for tumorigenesis of HCC cells. (a) The mRNA and protein levels of SF3B4 in Huh7 (left) and SMMC-7721(right) cells silencing SF3B4. (b) Cell proliferations were measured using CCK-8 assays in Huh7 (left) and SMMC-7721 (right) cells silencing SF3B4. (c) Cell proliferations were assessed using EdU immunofluorescence staining in Huh7 (left) and SMMC-7721(right) cells silencing SF3B4. Scale bars, 100 μm. (d) Cell migration was analyzed using transwell system in Huh7 (left) and SMMC-7721(right) cells silencing SF3B4. Scale bars, 100 μm. (e) Cell migration was analyzed using wound healing migration assays in Huh7 (left) and SMMC-7721(right) cells silencing SF3B4. Scale bars, 200 μm. Data is shown as mean with standard deviation (SD). $^{**}P < .01$, $^{*}P < .05$. Statistical analysis was determined by Student's *t*-test (a, b, c, d, e).

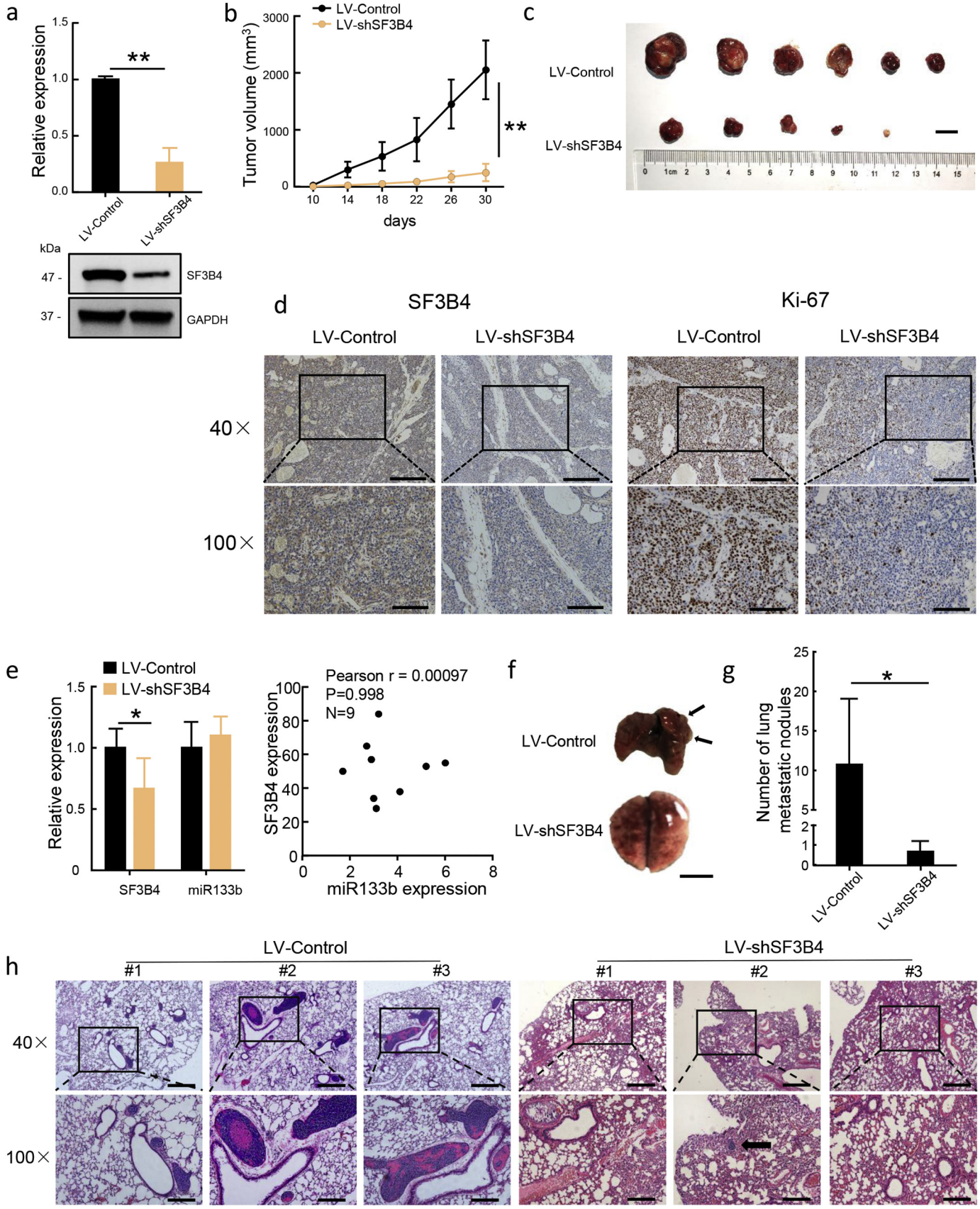

5-ethynyl-20- deoxyuridine (EdU) staining was used to measure the rate of proliferation of Huh7 and SMMC-7721 HCC cells (Fig. 3c). Results showed that SF3B4 knockdown significantly reduced growth of HCC and their proliferation rates. Transwell assays showed that SF3B4 was significantly associated with metastatic behavior of HCC cells. Cell counts of the SF3B4 knockdown group in lower chamber in transwell assays were found to be reduced by nearly 2-fold than those in the control group (Fig. 3d). Similarly, SF3B4 knockdown reduced the wound-

healing efficacy of HCC cells as measured using scratch wound healing assays (Fig. 3e).

To further confirm the effect of depleting SF3B4 in HCC, we depleted SF3B4 stably, using lentivirus shRNA (LV-shSF3B4) in Huh7 cells (Fig. 4a). Next, 3×10^6 LV-shSF3B4 Huh7 cells or control cells were injected into nude mice subcutaneously to measure tumor growth rate *in vivo*. Strikingly, depletion of SF3B4 significantly inhibited tumorigenesis of HCC cells *in vivo* (Fig. 4b, c). SF3B4 and Ki-67 staining of xenografts by IHC showed lighter staining density in LV-shSF3B4 group and further confirmed the critical role of SF3B4 (Fig. 4d). The transcription level was examined by q-PCR, which showed that SF3B4 expression is inhibited effectively in the LV-shSF3B4 group, whereas the expression of miRNA-133b does not show obvious differences in the LV-shSF3B4 and LV-control groups ($P = .4068$) (Fig. 4e, left). We further investigated the correlation of SF3B4 and miRNA-133b by Pearson correlation analysis and failed to find a significant relationship (Fig. 4e, right).

Furthermore, we injected 5×10^6 stably knocked-down SF3B4 HCC cells into the tail vein of nude mice to establish a lung metastatic model. We observed that the depletion of SF3B4 significantly inhibits metastatic colonization of HCC cells in lungs than that by the control group (Fig. 4f, g). Hematoxylin and eosin (HE) staining of mouse lung tissues showed that metastatic nodules in the SF3B4 depletion group are much smaller and fewer than those in the control group (Fig. 4h). Furthermore, we overexpressed SF3B4 in Huh7 and SMMC-7721 cells and found an increase in malignance of HCC cells (Fig. S2). These results revealed that SF3B4 plays a critical oncogenic role and SF3B4 knockdown inhibits proliferation and metastasis of HCC cells *in vitro and in vivo*.

3.4. MiRNA-133b plays an anti-cancer role by targeting SF3B4 in HCC cells

MiRNA-133b inhibits SF3B4 expression in HCC cells, which suggests that miRNA-133b may act as a tumor suppressor. The effect of miRNA-133b inhibition in HCC cells was examined to further investigate the molecular role of miRNA-133b (Fig. 5a). CCK8 and EdU assays showed that suppressing miRNA-133b expression using miRNA inhibitors increased proliferation of Huh7 (left) and SMMC-7721 (right) cells (Fig. 5b, c). The metastatic potential of HCC cells was examined using transwell and wound healing assays. We found that inhibiting miRNA-133b expression promoted metastasis of HCC cells, (Fig. 5d) and showed greater wound healing ability in HCC cells than that in control cells (Fig. 5e).

To further investigate whether miRNA-133b might affect the function of SF3B4 in HCC cells, we co-transfected miRNA-133b mimics and SF3B4 in SMMC-7721 cells, and the transfection efficiency was determined using real time RT-PCR and western blotting. As expected, overexpression of miRNA-133b in HCC cells inhibits SF3B4 expression at mRNA and protein levels (Fig. 6a). Then, we used CCK-8 and EdU assays to determine whether miRNA-133b mimics affect the growth and proliferation rates of SF3B4 overexpressed cells, and found that SMMC-7721 cells co-transfected with SF3B4 and miRNA-133b, show poor proliferation than SF3B4 overexpressed cells (Fig. 6b, c). Furthermore, miRNA-133b partly inhibits the migration of SF3B4 overexpressed cells, as seen using transwell and wound healing assays (Fig. 6d, e). Collectively, these results reveal that miRNA-133b is a tumor suppressor and miRNA-133b mimics can partly abolish the increased proliferation and migration abilities of SF3B4 overexpressed HCC cells.

3.5. MiRNA-133b inhibits liver cancer by modulating SF3B4 associated signaling pathways

Shen, et al. identified that SF3B4 overexpression activates the SF3b complex to splice wild type KLF4 into a non-functional transcript to promote tumorigenesis in HCC [11]. KLF4 is a conserved zinc finger-containing transcription factor that regulates multiple biological processes [24]. Recently, researchers found that KLF4 acts as a tumor suppressor in various human cancers, such as colorectal cancer, ovarian cancer, HCC, and lung cancer [25–28]. Overexpression of KLF4 recovers cyclin dependent kinase inhibitor 1B (KIP1) protein expression, a negative regulator of the cell cycle, and suppresses the epithelial-mesenchymal transition (EMT) protein, snail family transcriptional repressor 2 (SNAI2) in HCC cells [11]. To further investigate the association between miRNA-133b and the downstream targets of SF3B4, we altered the endogenous expression of miRNA-133b and SF3B4, then determined protein levels of KLF4, KIP1 and SNAI2 in HCC cells. Results showed that miRNA-133b overexpression has similar effects with SF3B4 knockdown, which promotes wild type KLF4 and KIP1 expression and inhibits SNAI2 expression (Fig. 7a left). Contrarily, inhibiting miRNA-133b suppressed KLF4 and KIP1 expression, and, increased SNAI2 expression (Fig. 7a right). These data provide evidence that miRNA-133b might regulate the SF3B4 associated signaling pathway to suppress HCC development (Fig. 7b).

4. Discussion

Splicing factors are major regulators of AS events and their aberrant expression or activity might result in dysregulation of splicing. SF3B4 is a member of the splicing factor 3b (SF3b) complex family. Prior studies have shown increased expression of SF3B4 and its diagnostic potential in HCC [9–11]. MiRNAs are an important class of small molecules in cellular processes and diseases [16,23,29]. However, the association between miRNAs and AS events is poorly understood. In this study, SF3B4-mediated regulation of proliferation and migration of HCC cells was consistent with previous observations showing that SF3B4 promotes the progression of HCC. Most importantly, our study suggests that miRNA-133b might be a novel negative regulator of SF3B4 in HCC. Overexpression of miRNA-133b partly eliminates the stimulatory effect of SF3B4 on proliferation and metastasis of HCC cells. Furthermore, expression of proteins of the SF3B4 pathway inversely correlates with that of miRNA-133b. Thus, MiRNA-133b appears to be a good target to inhibit HCC by suppressing the SF3B4 pathway.

The discovery of miRNAs as biologically relevant molecules has unraveled new possibilities of cellular and molecular complexities. In addition to the conventional regulatory mechanism of miRNAs, which post-transcriptionally decreases the levels of specific target genes, Dragomir et al. have summarized seven unconventional miRNA functions including coding for peptides, interacting with Non-AGO Proteins, activating Toll-like Receptors, upregulating protein expression, targeting mitochondrial transcripts, directly activating transcription, and targeting nuclear ncRNAs [30]. Several studies have assessed the regulation of splicing factors by miRNAs in cellular development and disease. MiRNA-222 inhibits the expression of Rbm24, a regulator of muscle-specific alternative splicing, which leads to the alteration of myogenic differentiation [31]. Researchers found that miRNA-124 promotes nervous system (NS) development by directly targeting PTBP1,

Fig. 4. SF3B4 knockdown suppressed the tumor growth and metastasis *in vivo*. (a) The mRNA and protein levels of SF3B4 in SF3B4 stably silenced Huh7 cells. LV-shSF3B4, recombinant lentivirus suppressing SF3B4, LV-Control, recombinant lentivirus negative control. (b) Effects of SF3B4 depletion in Huh7 cells on subcutaneous tumor growth. Tumor volumes were measured every 4 days when there is a subcutaneous tumor growing in mice. (c) The mice were killed at 30 days after injection, and the tumors were excised. $n = 6$ mice in each group. Scale bars, 10 mm. (d) IHC analysis examining SF3B4 (left) and Ki-67 (right) protein levels in mice xenografts. Scale bars, 200 μm (top), 100 μm (bottom). (e) Left: The expression levels of SF3B4 and miRNA-133b in xenografts were examined by q-PCR. Right: The correlation between SF3B4 and miRNA-133b expression levels in xenografts. (f) The *in vivo* metastasis of HCC cell line stably suppressing SF3B4 was examined. The mice were killed and the lung was visualized 5 weeks post-transplantation. n = 6 mice in each group. Scale bars, 5 mm. (g) Lung metastatic nodules of mice were counted in each group. (h) Histopathological analysis of pulmonary metastases in the mouse model was conducted using hematoxylin and eosin (HE) staining. Scale bars, 200 μm (top), 100 μm (bottom). Data is shown as mean with standard deviation (SD). $^{**}P < .01$, $^{*}P < .05$. Statistical analysis was determined by Student's *t*-test (a, b, e left, g) and Pearson correlation analysis (e right).

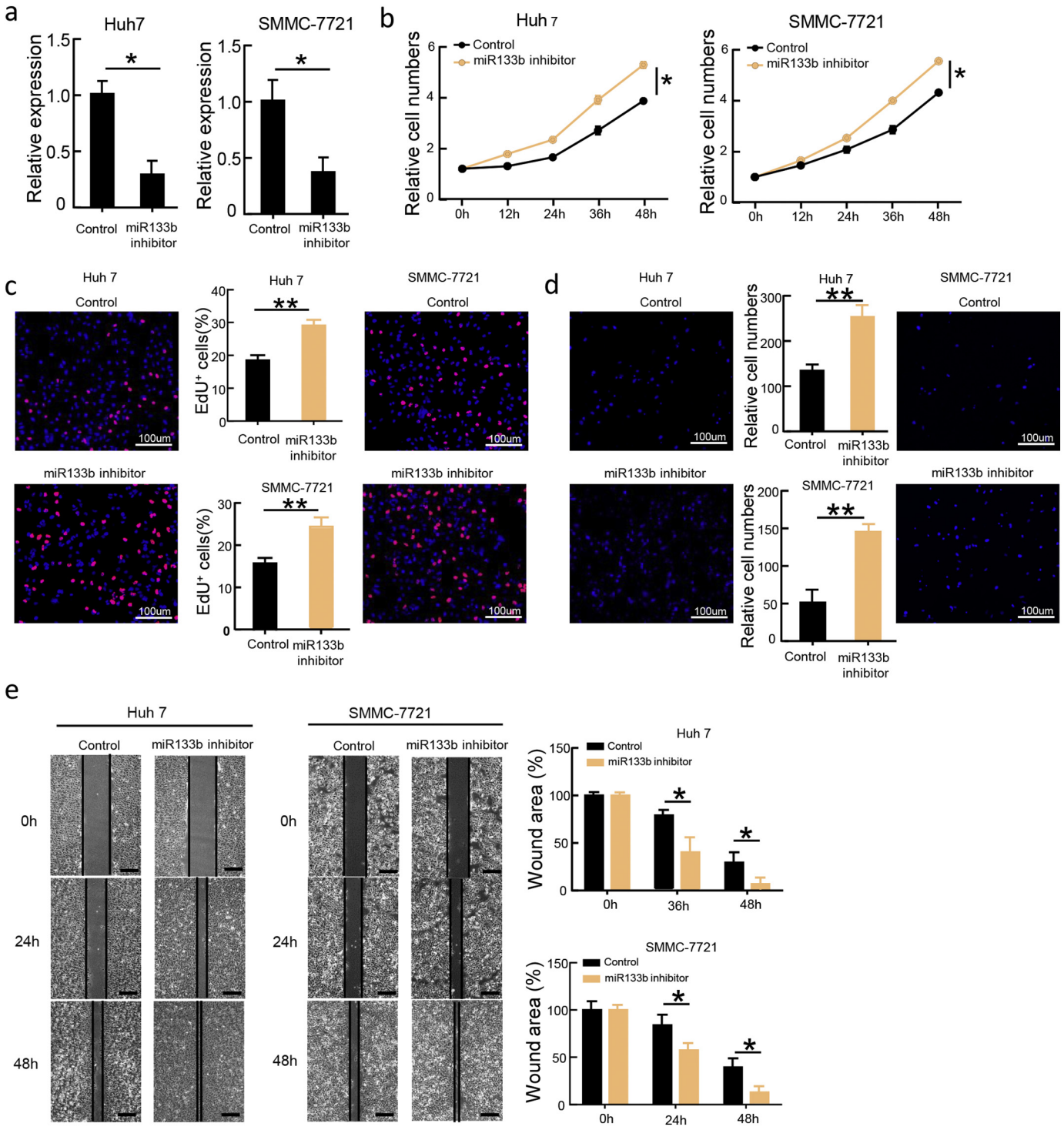

Fig. 5. MiRNA-133b acts as a tumor suppressor in HCC. (a) The expression levels of miRNA-133b in Huh7 (left) and SMMC-7721(right) cells inhibiting miRNA-133b. (b) Cell proliferations were measured using CCK-8 assays in Huh7 (left) and SMMC-7721 (right) cells inhibiting miRNA-133b. (c) Cell proliferations were assessed using EdU immunofluorescence staining in Huh7 (left) and SMMC-7721(right) cells inhibiting miRNA-133b. Scale bars, 100 μm. (d) Cell migration was analyzed using transwell system in Huh7 (left) and SMMC-7721(right) cells inhibiting miRNA-133b. Scale bars, 100 μm. (e) Cell migration was analyzed using wound healing migration assays in Huh7 (left) and SMMC-7721(right) cells inhibiting miRNA-133b. Scale bars, 200 μm. Data is shown as mean with standard deviation (SD). $^{**}P < .01$, $^{*}P < .05$. Statistical analysis was determined by Student's t-test (a, b, c, d, e).

a suppressor of NS-specific splicing [32]. In renal cancer cells, Boguslawska et al. found that SRSF7 is regulated by miRNA-126b. They also found a regulatory feedback loop between SRSF7 and miRNAs in which the expression of miR-30a-5p and miR-181a-5p was regulated by their target, SRSF7 [33]. In our study, we did not find the feedback effect of SF3B4 on miRNA-133b either *in vitro* or *in vivo*, possibly because the regulatory mechanism of miRNA-133b/SF3B4 axis is unidirectional and miRNA-133b is an upstream molecular regulator of SF3B4.

Recently, investigators have shown that miRNA-133b has different target genes and plays a vital role in various human tumors [34–38]. In human non-small cell lung cancers (NSCLC), miRNA-133b inhibited cell growth, migration, and invasion by targeting matrix metallopeptidase 9

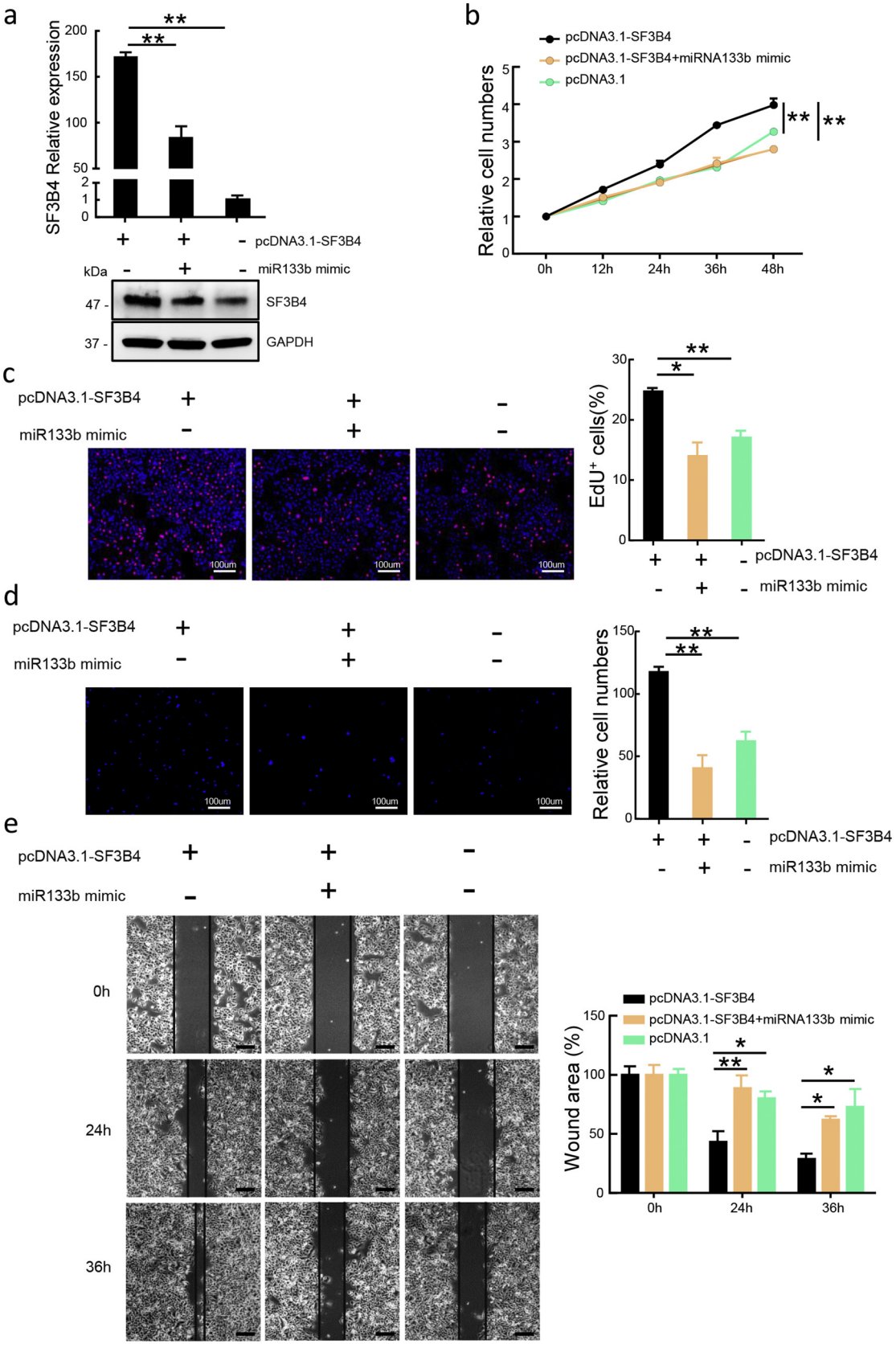

Fig. 6. MiRNA-133b abolish the tumorigenesis effects of SF3B4. (a) The mRNA and protein levels of SF3B4 in Huh7 cells overexpressing SF3B4 and co-transfecting with miRNA-133b mimic. (b) Cell proliferations were measured using CCK-8 assays in Huh7 cells overexpressing SF3B4 and co-transfecting with miRNA-133b mimic. (c) Cell proliferations were assessed using EdU immunofluorescence staining (top) and cell migration was analyzed using transwell system (bottom) in Huh7 cells overexpressing SF3B4 and co-transfecting with miRNA-133b mimic. Scale bars, 100 μm. (d) Cell migration was analyzed using wound healing migration assays in Huh7 cells overexpressing SF3B4 and co-transfecting with miRNA-133b mimic. Scale bars, 200 μm. Data is shown as mean with standard deviation (SD). **P < .01, *P < .05. Statistical analysis was determined by Student's t-test (a, b, c, d, e).

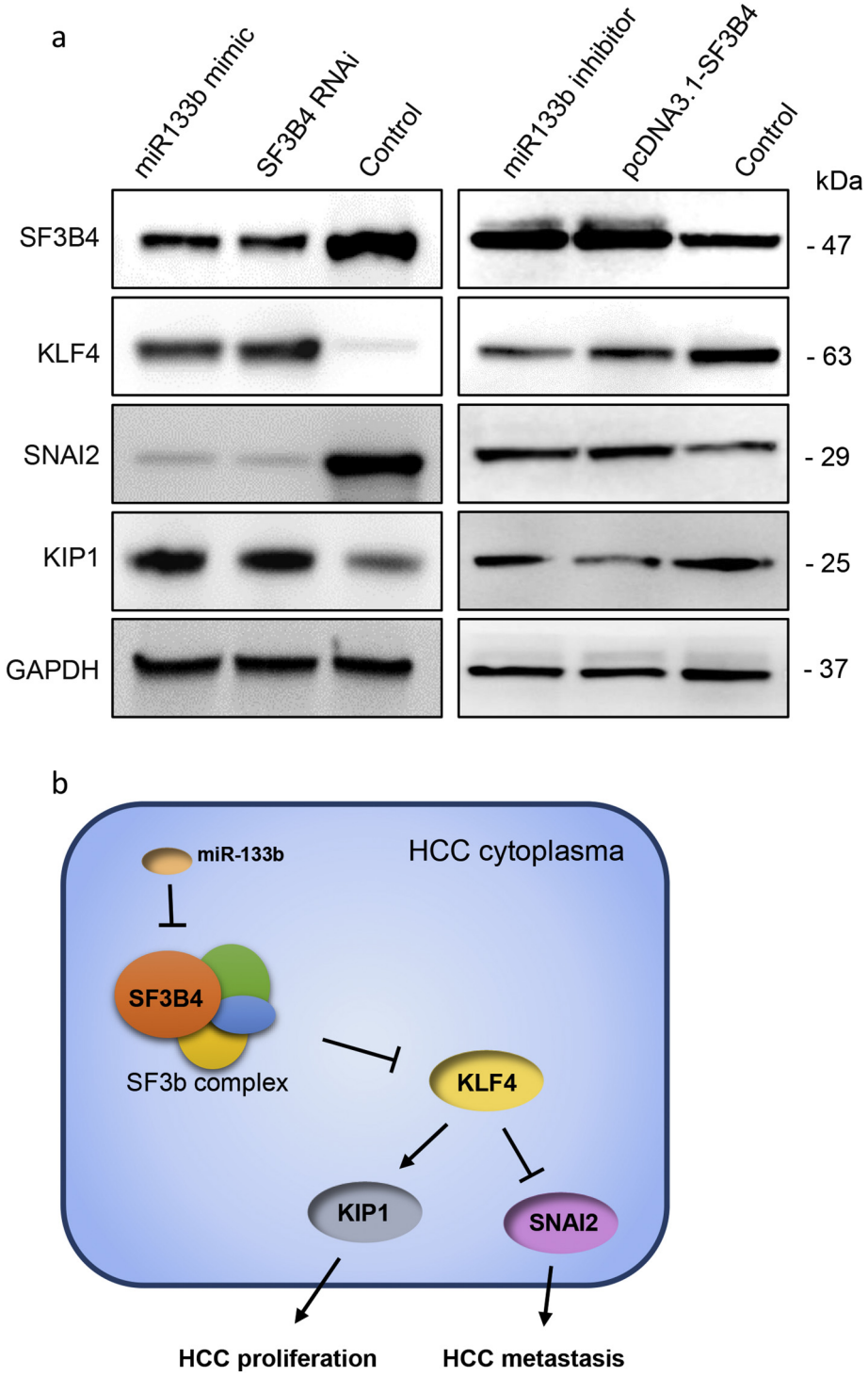

Fig. 7. MiRNA-133b modulates SF3B4 associated signal pathway. (a) The protein levels of SF3B4 and associated downstream targets when transfected with miRNA-133b mimic or SF3B4 siRNA (left) as well as overexpressed SF3B4 or transfected with miRNA-133b inhibitor (right). (b) Proposed schematic illustrating oncogenic function and regulatory mechanism of SF3B4 in HCC.

(MMP9) [34]. Overexpression of miRNA-133b in glioma cell lines suppresses silent information regulator 1 (Sirt1) and reduces the proliferation and invasion of U87 cells [36]. Similarly, our study suggests that miRNA-133b overexpression decreases the growth and metastasis of HCC cells by affecting the expression of members of the SF3B4 pathway. However, our findings with respect to the biological functions and the correlation of SF3B4 and miRNA-133b were only tested in HCC cells. Whether this inverse relationship exists between SF3B4 and miRNA-133b, can be examined using other human solid tumors.

In a conclusion, our study provides evidence that SF3B4 is upregulated and plays a critical role in HCC. Meanwhile, a compelling inverse correlation between SF3B4 and miRNA-133b has been revealed in this study. MiRNA-133b not only regulates the endogenous expression of SF3B4 but also modulates SF3B4-mediated AS efficiency in HCC tumorigenesis. These results indicate that the miRNA-133b/SF3B4 axis may serve as potential therapeutic target for the treatment of HCC.

Supplementary data to this article can be found online at https://doi.org/10.1016/j.ebiom.2018.10.067.

Acknowledgements

We thank for the support from Dr. Jingjing Hu in technical help.

Funding sources

This work was supported by the grants of China National Funds for Distinguished Young Scientists (No.81425019), the State Key Program of National Natural Science Foundation of China (No.81730076), Shanghai Science and Technology Committee Program (No.18XD1405300) and Specially-Appointed Professor Fund of Shanghai (GZ2015009). China National Funds for National Natural Science Fund (No. 81672899).

Conflicts of interest

The authors declare no conflicts of interest.

Author contributions

Concept and design of study: Zhiyong Liu and Shanrong Liu.
Performed the experiments: Zhiyong Liu, Wei Li and Yanan Pang.
Data analysis and interpretation: Zhiyong Liu, Zaixin Zhou, Shupeng Liu and Kai Cheng, Qin Qin and Yin Jia.
Supervision: Shanrong Liu.
Manuscript writing: All authors.
Final approval of manuscript: All authors.
Accountable for all aspects of the work: All authors.

References

[1] Siegel RL, Miller KD, Jemal A. Cancer Statistics, 2017. CA Cancer J Clin 2017;67(1):7–30.
[2] Bruix J, Gores GJ, Mazzaferro V. Hepatocellular carcinoma: Clinical frontiers and perspectives. Gut 2014;63(5):844–55.
[3] Lee JS, Lin YY, Wang TS, Liu JY, Lin WW, Yang JJ. Antitumorigenic Effects of ZAKbeta, an Alternative Splicing Isoform of ZAK. Chin J Physiol 2018;61(1):25–34.
[4] Yuan JH, Liu XN, Wang TT, Pan W, Tao QF, Zhou WP, et al. The MBNL3 splicing factor promotes hepatocellular carcinoma by increasing PXN expression through the alternative splicing of lncRNA-PXN-AS1. Nat Cell Biol 2017;19(7):820–32.
[5] Li J, Wang Y, Rao X, Wang Y, Feng W, Liang H, et al. Roles of alternative splicing in modulating transcriptional regulation. BMC Syst Biol 2017;11(Suppl. 5):89.
[6] Golas MM, Sander B, Will CL, Luhrmann R, Stark H. Molecular architecture of the multiprotein splicing factor SF3b. Science 2003;300(5621):980–4.
[7] Cassina M, Cerqua C, Rossi S, Salviati L, Martini A, Clementi M, et al. A synonymous splicing mutation in the SF3B4 gene segregates in a family with highly variable Nager syndrome. Eur J Hum Genet 2017;25(3):371–5.
[8] Petit F, Escande F, Jourdain AS, Porchet N, Amiel J, Doray B, et al. Nager syndrome: Confirmation of SF3B4 haploinsufficiency as the major cause. Clin Genet 2014;86(3):246–51.
[9] Iguchi T, Komatsu H, Masuda T, Nambara S, Kidogami S, Ogawa Y, et al. Increased Copy Number of the Gene Encoding SF3B4 Indicates Poor Prognosis in Hepatocellular Carcinoma. Anticancer Res 2016;36(5):2139–44.
[10] Xu W, Huang H, Yu L, Cao L. Meta-analysis of gene expression profiles indicates genes in spliceosome pathway are up-regulated in hepatocellular carcinoma (HCC). Med Oncol 2015;32(4):96.
[11] Shen Q, Eun JW, Lee K, Kim HS, Yang HD, Kim SY, et al. BANF1, PLOD3, SF3B4 as Early-stage Cancer Decision Markers and Drivers of Hepatocellular Carcinoma. Hepatology 2018;67(4):1360–77.
[12] Alvarez-Garcia I, Miska EA. MicroRNA functions in animal development and human disease. Development 2005;132(21):4653–62.
[13] Sun CC, Li SJ, Yuan ZP, Li DJ. MicroRNA-346 facilitates cell growth and metastasis, and suppresses cell apoptosis in human non-small cell lung cancer by regulation of XPC/ERK/Snail/E-cadherin pathway. Aging (Albany NY) 2016;8(10):2509–24.
[14] Friedman RC, Farh KK, Burge CB, Bartel DP. Most mammalian mRNAs are conserved targets of microRNAs. Genome Res 2009;19(1):92–105.
[15] Zhang ZW, Chen JJ, Xia SH, Zhao H, Yang JB, Zhang H, et al. Long intergenic non-protein coding RNA 319 aggravates lung adenocarcinoma carcinogenesis by modulating miR-450b-5p/EZH2. Gene 2018;650:60–7.
[16] Sun CC, Zhang L, Li G, Li SJ, Chen ZL, Fu YF, et al. The lncRNA PDIA3P Interacts with miR-185-5p to Modulate Oral Squamous Cell Carcinoma Progression by Targeting Cyclin D2. Mol Ther Nucleic Acids 2017;9:100–10.
[17] Sun C, Li S, Zhang F, Xi Y, Wang L, Bi Y, et al. Long non-coding RNA NEAT1 promotes non-small cell lung cancer progression through regulation of miR-377-3p-E2F3 pathway. Oncotarget 2016;7(32):51784–814.
[18] Rahmani F, Avan A, Hashemy SI, Hassanian SM. Role of Wnt/beta-catenin signaling regulatory microRNAs in the pathogenesis of colorectal cancer. J Cell Physiol 2018;233(2):811–7.
[19] Perrotti D, Eiring AM. The new role of microRNAs in cancer. Future Oncol 2010;6(8):1203–6.
[20] Peng Y, Croce CM. The role of MicroRNAs in human cancer. Signal Transduct Target Ther 2016;1:15004.
[21] Sun C, Li S, Yang C, Xi Y, Wang L, Zhang F, et al. MicroRNA-187-3p mitigates non-small cell lung cancer (NSCLC) development through down-regulation of BCL6. Biochem Biophys Res Commun 2016;471(1):82–8.
[22] Tang Z, Li C, Kang B, Gao G, Li C, Zhang Z. GEPIA: A web server for cancer and normal gene expression profiling and interactive analyses. Nucleic Acids Res 2017;45(W1):W98–w102.
[23] Burchard J, Zhang C, Liu AM, Poon RT, Lee NP, Wong KF, et al. microRNA-122 as a regulator of mitochondrial metabolic gene network in hepatocellular carcinoma. Mol Syst Biol 2010;6:402.
[24] Ghaleb AM, Yang VW. Kruppel-like factor 4 (KLF4): what we currently know. Gene 2017;611:27–37.
[25] Liu S, Yang H, Chen Y, He B, Chen Q. Kruppel-like factor 4 Enhances Sensitivity of Cisplatin to Lung Cancer Cells and Inhibits Regulating Epithelial-to-Mesenchymal transition. Oncol Res 2016;24(2):81–7.
[26] Xiu DH, Chen Y, Liu L, Yang HS, Liu GF. Tumor-suppressive role of Kruppel-like factor 4 (KLF-4) in colorectal cancer. Genet Mol Res 2017;16(1).
[27] Wang B, Shen A, Ouyang X, Zhao G, Du Z, Huo W, et al. KLF4 expression enhances the efficacy of chemotherapy drugs in ovarian cancer cells. Biochem Biophys Res Commun 2017;484(3):486–92.
[28] Sun H, Peng Z, Tang H, Xie D, Jia Z, Zhong L, et al. Loss of KLF4 and consequential downregulation of Smad7 exacerbate oncogenic TGF-beta signaling in and promote progression of hepatocellular carcinoma. Oncogene 2017;36(21):2957–68.
[29] Sun CC, Li SJ, Zhang F, Zhang YD, Zuo ZY, Xi YY, et al. The Novel miR-9600 Suppresses Tumor Progression and Promotes Paclitaxel Sensitivity in Non-small-cell Lung Cancer through Altering STAT3 Expression. Mol Ther Nucleic Acids 2016;5(11):e387.
[30] Dragomir MP, Knutsen E, Calin GA. SnapShot: Unconventional miRNA Functions. Cell 2018;174(4):1038.
[31] Cardinali B, Cappella M, Provenzano C, Garcia-Manteiga JM, Lazarevic D, Cittaro D, et al. MicroRNA-222 regulates muscle alternative splicing through Rbm24 during differentiation of skeletal muscle cells. Cell Death Dis 2016;7:e2086.
[32] Makeyev EV, Zhang J, Carrasco MA, Maniatis T. The MicroRNA miR-124 promotes neuronal differentiation by triggering brain-specific alternative pre-mRNA splicing. Mol Cell 2007;27(3):435–48.
[33] Boguslawska J, Sokol E, Rybicka B, Czubaty A, Rodzik K, Piekielko-Witkowska A. microRNAs target SRSF7 splicing factor to modulate the expression of osteopontin splice variants in renal cancer cells. Gene 2016;595(2):142–9.
[34] Zhen Y, Liu J, Huang Y, Wang Y, Li W, Wu J. miR-133b Inhibits Cell Growth, Migration, and Invasion by Targeting MMP9 in Non-Small Cell Lung Cancer. Oncol Res 2017;25(7):1109–16.
[35] Sugiyama T, Taniguchi K, Matsuhashi N, Tajirika T, Futamura M, Takai T, et al. MiR-133b inhibits growth of human gastric cancer cells by silencing pyruvate kinase muscle-splicer polypyrimidine tract-binding protein 1. Cancer Sci 2016;107(12):1767–75.
[36] Li C, Liu Z, Yang K, Chen X, Zeng Y, Liu J, et al. miR-133b inhibits glioma cell proliferation and invasion by targeting Sirt1. Oncotarget 2016;7(24):36247–54.
[37] Li B, Ding CM, Li YX, Peng JC, Geng N, Qin WW. Over-regulation of microRNA-133b inhibits cell proliferation of cisplatin-induced non-small cell lung cancer cells through PI3K/Akt and JAK2/STAT3 signaling pathway by targeting EGFR. Oncol Rep 2018;39(3):1227–34.
[38] Wang X, Bu J, Liu X, Wang W, Mai W, Lv B, et al. miR-133b suppresses metastasis by targeting HOXA9 in human colorectal cancer. Oncotarget 2017;8(38):63935–48.